INTERNATIONAL JOURNAL FOR NUMERICAL METHODS IN FLUIDS
Int. J. Numer. Meth. Fluids 2003; **41**:695–719 (DOI: 10.1002/fld.462)

Relaxation schemes for the shallow water equations

A. I. Delis[1,*] and Th. Katsaounis[2]

[1] *Department of Applied Mathematics, University of Crete, Heraklion 71409, Crete, Greece*
[2] *Departement de Mathématiques et Applications, Ecole Normale Supérieure, Paris 75230, France*

SUMMARY

We present a class of first and second order in space and time relaxation schemes for the shallow water (SW) equations. A new approach of incorporating the geometrical source term in the relaxation model is also presented. The schemes are based on classical relaxation models combined with Runge–Kutta time stepping mechanisms. Numerical results are presented for several benchmark test problems with or without the source term present. Copyright © 2003 John Wiley & Sons, Ltd.

KEY WORDS: relaxation schemes; swallow water equations; finite differences

1. INTRODUCTION

We consider the well known one-dimensional shallow water (SW) system, with a geometrical source term (the bottom topography) added, written in differential conservation law form as a single vector equation

$$\mathbf{U}_t + \mathbf{F}(\mathbf{U})_x = \mathbf{S}(\mathbf{U}) \tag{1}$$

with

$$\mathbf{U} = \begin{bmatrix} h \\ hu \end{bmatrix}, \quad \mathbf{F}(\mathbf{U}) = \begin{bmatrix} hu \\ hu^2 + \frac{g}{2}h^2 \end{bmatrix}, \quad \mathbf{S}(\mathbf{U}) = \begin{bmatrix} 0 \\ -ghZ' \end{bmatrix}$$

System (1) describes the flow at time $t \geqslant 0$ at point $x \in \mathbb{R}$, where $h(x,t) \geqslant 0$ is the total water height above the bottom, $u(x,t)$ is the average horizontal velocity, $Z(x)$ is the bottom height function (see Figure 1) and g the gravitational acceleration.

The SW equations (1) are a hyperbolic system with a source term, due to the topography of the bottom, with unknown quantities h, u. In the homogeneous case, the system is equivalent to that of isentropic Euler system. However due to the presence of the source term the properties of the system change substantially. The above system is quite simple in the sense that only

* Correspondence to: A. I. Delis, Department of Applied Mathematics, University of Crete, Heraklion 71409, Crete, Greece.

Received February 2002
Revised 15 July 2002

Copyright © 2003 John Wiley & Sons, Ltd.

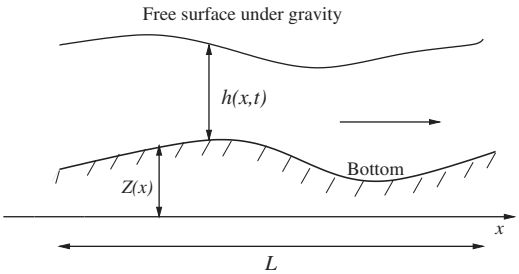

Figure 1. Shallow flow.

the topography of the bottom in taken into account, but other terms could be also added in order to include effects such as friction on the bottom and on the surface as well as variations of the channel width.

A wide variety of physical phenomena are governed by the SW equations. An important class of problems of practical interest involve water flows, including tidal flows in estuary and coastal water regions, bore wave propagation, flood waves in rivers, surges and dam-break modelling among others. The inclusion of source terms, e.g. those terms relevant to bottom topography is often necessary to permit the modelling of such realistic problems.

In recent years many methods were proposed for the numerical approximation of solutions of hyperbolic conservations laws with source terms. The main difficulty being here, the numerical treatment of the source terms. Finite volume methods are widely used, and in particular the well balanced schemes introduced by Greenberg and LeRoux, [1], Gosse and LeRoux [2] and recently Gosse [3, 4] extended the idea for hyperbolic systems of balance laws and in SW equations as in Reference [5]. Another approach is the Godunov type schemes presented in References [6, 7] and the approach, which does not modify the Godunov solver, but approximates the source term in an upwind fashion using local characteristic decomposition, that was introduced in References [8–10]. The application of central-upwind schemes to shallow water systems with source terms has also been presented in Reference [11]. The most important property of all these schemes is that they are designed in order to preserve steady states, as accurately as possible, one of the main characteristics of the continuous model.

Another class of schemes were introduced in Reference [12]. These schemes are based on the kinetic interpretation of the system. An entropy satisfying kinetic scheme which also preserves the steady states in presented in Reference [13].

In this work we consider finite difference relaxation schemes for (1). This class of relaxation schemes was first introduced in Reference [14] and subsequently have been recently widely applied and studied, see for example [15–21]. Recently in Reference [22] the connection between a simple relaxation scheme of the type proposed in Reference [14] and a class of approximate Riemann solvers has been explored.

The relaxation scheme that includes a source term was used in Reference [23] for flows in open channel networks by solving the Saint Venant equations. An analysis of a class of relaxation schemes for hyperbolic conservation laws with stiff source terms is presented in Reference [24]. In this work, we utilize the classical relaxation type of schemes, with a novel treatment of the source term, which combine finite volume shock capturing spatial

Copyright © 2003 John Wiley & Sons, Ltd.

discretizations that are Riemann solver free, and a Runge–Kutta method that provides the time stepping mechanisms. The proposed schemes combine simplicity and high efficiency. Their performance in various test problems shows that they can provide a reliable alternative for shallow water wave computations. A non standard relaxation model is used in computations of steady state regimes with very promising results.

This paper is organized as follows: The relaxation systems for two different treatments of the source term for the SW equations are introduced in Section 2. The semi-discrete first and second order schemes are presented in Section 3. Section 4 is devoted in the presentation of the fully discrete schemes. Finally, in Section 5 a series of experiments displaying the features of the methods are presented.

2. RELAXATION SYSTEMS FOR THE SW EQUATIONS

Relaxation systems for the SW equations are motivated by the relaxation system of [14] for the 1-D scalar conservation laws. Indeed, if we consider the classical 1-D conservation law

$$\begin{aligned} u_t + f(u)_x = 0, \quad x \in \mathbb{R},\ t > 0 \\ u(x,0) = u_0(x), \quad x \in \mathbb{R} \end{aligned} \tag{2}$$

then the relaxation system of Reference [14] reads as follows:

$$\begin{aligned} u_t + v_x &= 0 \\ v_t + c^2 u_x &= -\frac{1}{\varepsilon}(v - f(u)) \end{aligned} \tag{3}$$

If the *subcharateristic condition*: $|f'(u)| < c$ holds true then in the relaxation limit $\varepsilon \to 0$ we recover (2).

Following this previous motivation we write a relaxation system for the SW equations replacing the conservation law (1) by a larger system. Indeed we write, with $q = hu$,

$$h_t + v_x = 0 \tag{4a}$$

$$q_t + w_x = -ghZ' \tag{4b}$$

$$v_t + c_1^2 h_x = -\frac{1}{\varepsilon}(v - q) \tag{4c}$$

$$w_t + c_2^2 q_x = -\frac{1}{\varepsilon}\left(w - \left(\frac{q^2}{h} + \frac{g}{2}h^2\right)\right) \tag{4d}$$

by setting now

$$\mathbf{u} = \begin{bmatrix} h \\ q \end{bmatrix}, \quad \mathbf{v} = \begin{bmatrix} v \\ w \end{bmatrix} \tag{5}$$

Copyright © 2003 John Wiley & Sons, Ltd.

system (4) can be rewritten as

$$\begin{aligned} \mathbf{u}_t + \mathbf{v}_x &= \mathbf{S}(\mathbf{u}) \\ \mathbf{v}_t + \mathbf{C}^2\mathbf{u}_x &= -\frac{1}{\varepsilon}(\mathbf{v} - \mathbf{F}(\mathbf{u})) \end{aligned} \tag{6}$$

where now $\mathbf{u}, \mathbf{v} \in \mathbb{R}^2$ and $\mathbf{C}^2 \in \mathbb{R}^{2\times 2}$ is a positive matrix. We assume without loss of generality that $\mathbf{C}$ has positive eigenvalues $c_j > 0$ for $j = 1, 2$.

System (6) can now be further reformulated as

$$\begin{bmatrix} \mathbf{u} \\ \mathbf{v} \end{bmatrix}_t + \begin{bmatrix} 0 & \mathbf{I} \\ \mathbf{C}^2 & 0 \end{bmatrix} \begin{bmatrix} \mathbf{u} \\ \mathbf{v} \end{bmatrix}_x = \begin{bmatrix} \mathbf{S}(\mathbf{u}) \\ -\frac{1}{\varepsilon}(\mathbf{v} - \mathbf{F}(\mathbf{u})) \end{bmatrix} \tag{7}$$

We also consider a variant of the above relaxation system which reads, see Reference [25] for a derivation, as

$$h_t + v_x = 0 \tag{8a}$$

$$q_t + w_x = 0 \tag{8b}$$

$$v_t + c_1^2 h_x = -\frac{1}{\varepsilon}(v - q) \tag{8c}$$

$$w_t + c_2^2 q_x = -\frac{1}{\varepsilon}\left(w - \left(\frac{q^2}{h} + \frac{g}{2}h^2\right)\right) + \frac{1}{\varepsilon}\int^x gh(y)Z'(y)\,\mathrm{d}y \tag{8d}$$

or written in vector form as

$$\begin{bmatrix} \mathbf{u} \\ \mathbf{v} \end{bmatrix}_t + \begin{bmatrix} 0 & \mathbf{I} \\ \mathbf{C}^2 & 0 \end{bmatrix} \begin{bmatrix} \mathbf{u} \\ \mathbf{v} \end{bmatrix}_x = \begin{bmatrix} 0 \\ -\frac{1}{\varepsilon}(\mathbf{v} - \mathbf{F}(\mathbf{u})) - \frac{1}{\varepsilon}\tilde{\mathbf{S}}(\mathbf{u}) \end{bmatrix} \tag{9}$$

where

$$\tilde{\mathbf{S}}(\mathbf{u}) = \begin{bmatrix} 0 \\ -\int^x gh(y)Z'(y)\,\mathrm{d}y \end{bmatrix}$$

The original conservation law has now, in both formulations, been replaced by a linear hyperbolic system with a relaxation source term which rapidly drives $\mathbf{v} \to \mathbf{F}(\mathbf{u})$ in the relaxation limit $\varepsilon \to 0$. In some cases it can be shown analytically that solutions to (7) approach solutions to the original conservation law. See for example References [26–30], for discussions of this condition and convergence properties.

A general necessary condition for such convergence is that the subcharacteristic condition is satisfied. For systems (7), (9) we require that every eigenvalue λ of $\mathbf{F}'(\mathbf{u})$ satisfies

$$|\lambda| \leqslant c_{\max} \tag{10}$$

where $c_{\max} = \max_j c_j$. By doing so we insure that the characteristic speeds of the hyperbolic part of (7) or (9) are at least as large as the characteristic speeds of the original problem.

Copyright © 2003 John Wiley & Sons, Ltd.

Hence, by choosing the constants c_1, c_2 appropriately, so that the corresponding subcharacteristic conditions hold true, in the relaxation limit $\varepsilon \to 0$ we recover (1), for both relaxation systems (7) and (9). Notice that in the case where $Z \equiv 0$ then the two schemes are identical.

3. SEMI-DISCRETE RELAXATION SCHEMES

We start first with the semi-discrete schemes for the relaxation systems (7) and (9). We consider a classical first order upwind scheme and a second order MUSCL scheme. For brevity we present the semi-discrete schemes for system (7).

To discretize the system of equations (7) we assume a uniform spaced grid with $\Delta x = x_{i+(1/2)} - x_{i-(1/2)}$ and a uniform time step $\Delta t = t^{n+1} - t^n$, $n = 0, 1, 2, \ldots$. The approximate solution, denoted as the discrete value $\mathbf{u}_i^n$, is the approximate cell average of the variable $\mathbf{u}$ in the cell $(x_{i+1/2}, x_{i-1/2})$ at time $t = t^n$. The approximate point value of $\mathbf{u}$ at $x = x_{i+1/2}$ at time $t = t^n$ is denoted by $\mathbf{u}_{i+1/2}^n$.

3.1. The upwind scheme

We start by considering the following one-step conservative system for the homogeneous case (no source term present):

$$\begin{aligned} \frac{\partial}{\partial t}\mathbf{u}_i + \frac{1}{\Delta x}(\mathbf{v}_{i+1/2} - \mathbf{v}_{i-1/2}) &= 0 \\ \frac{\partial}{\partial t}\mathbf{v}_i + \frac{1}{\Delta x}\mathbf{C}^2(\mathbf{u}_{i+1/2} - \mathbf{u}_{i-1/2}) &= -\frac{1}{\varepsilon}(\mathbf{v}_i - \mathbf{F}(\mathbf{u}_i)) \end{aligned} \tag{11}$$

The linear hyperbolic part of the (11) has two Riemann invariants (characteristic speeds)

$$\mathbf{v} \pm \mathbf{C}\mathbf{u}$$

associated with the characteristic fields $\pm\mathbf{C}$, respectively. The first order upwind approximation of $\mathbf{v} \pm \mathbf{C}\mathbf{u}$ reads

$$(\mathbf{v} + \mathbf{C}\mathbf{u})_{i+1/2} = (\mathbf{v} + \mathbf{C}\mathbf{u})_i, \quad (\mathbf{v} - \mathbf{C}\mathbf{u})_{i+1/2} = (\mathbf{v} - \mathbf{C}\mathbf{u})_{i+1} \tag{12}$$

Hence

$$\begin{aligned} \mathbf{u}_{i+1/2} &= \tfrac{1}{2}(\mathbf{u}_i + \mathbf{u}_{i+1}) - \tfrac{1}{2}\mathbf{C}^{-1}(\mathbf{v}_{i+1} - \mathbf{v}_i) \\ \mathbf{v}_{i+1/2} &= \tfrac{1}{2}(\mathbf{v}_i + \mathbf{v}_{i+1}) - \tfrac{1}{2}\mathbf{C}(\mathbf{u}_{i+1} - \mathbf{u}_i) \end{aligned} \tag{13}$$

We can then construct the following first order upwind semi-discrete approximation of the relaxation scheme (9):

$$\begin{aligned} \frac{\partial}{\partial t}\mathbf{u}_i + \frac{1}{2\Delta x}(\mathbf{v}_{i+1} - \mathbf{v}_{i-1}) - \frac{1}{2\Delta x}\mathbf{C}(\mathbf{u}_{i+1} - 2\mathbf{u}_i + \mathbf{u}_{i-1}) &= 0 \\ \frac{\partial}{\partial t}\mathbf{v}_i + \frac{1}{2\Delta x}\mathbf{C}^2(\mathbf{u}_{i+1} - \mathbf{u}_{i-1}) - \frac{1}{2\Delta x}\mathbf{C}(\mathbf{v}_{i+1} - 2\mathbf{v}_i + \mathbf{v}_{i-1}) &= -\frac{1}{\varepsilon}(\mathbf{v}_i - \mathbf{F}(\mathbf{u}_i)) - \frac{1}{\varepsilon}\tilde{\mathbf{S}}(\mathbf{u}_i) \end{aligned} \tag{14}$$

Copyright © 2003 John Wiley & Sons, Ltd.

where now

$$\tilde{\mathbf{S}}(\mathbf{u}_i) = \begin{bmatrix} 0 \\ -\int^{x_i} gh(y)Z'(y)\,\mathrm{d}y \end{bmatrix}$$

3.2. A MUSCL scheme

To construct a second order accurate in space scheme, the piecewise constant approximation (12) is replaced with a MUSCL piecewise linear interpolation which, applied to the kth component of $\mathbf{v} \pm \mathbf{C}\mathbf{u}$, gives, respectively:

$$\begin{aligned} (v + c_k u)_{i+(1/2)} &= (v + c_k u)_i + \tfrac{1}{2}\Delta x s_i^+ \\ (v - c_k u)_{i+(1/2)} &= (v - c_k u)_{i+1} - \tfrac{1}{2}\Delta x s_{i+1}^- \end{aligned} \tag{15}$$

where u, v are the kth ($1 \leqslant k \leqslant 2$ for the SW equations) components of $\mathbf{v}, \mathbf{u}$ respectively, and the slopes $s^{\pm}$ in the ith cell are defined by

$$s_i^{\pm} = \frac{1}{\Delta x}(v_{i+1} \pm c_k u_{i+1} - v_i \mp c_k u_i)\phi(\theta_i^{\pm}) \tag{16}$$

with

$$\theta_i^{\pm} = \frac{v_i \pm c_k u_i - v_{i-1} \mp c_k u_{i-1}}{v_{i+1} \pm c_k u_{i+1} - v_i \mp c_k u_i} \tag{17}$$

where ϕ is a limiter function, as defined for example by Sweby [31], satisfying

$$0 \leqslant \phi(\theta) \leqslant \mathrm{minmod}(2, 2\theta) \tag{18}$$

There are several options on choosing a limiter function. Some of the most popular ones are, the MinMod (MM) limiter

$$\phi(\theta) = \max(0, \min(1, \theta))$$

the VanLeer (VL) limiter

$$\phi(\theta) = \frac{|\theta| + \theta}{1 + |\theta|}$$

and the Monotonized Central (MC) limiter

$$\phi(\theta) = \max(0, \min((1 + \theta)/2, 2, 2\theta))$$

The last two limiters have been shown to exhibit sharper resolution of discontinuities, since they do not reduce the slope as severely as MM near a discontinuity. It should be noted here that (18) provides sufficient bounds on the flux limiters for the TVD condition to be satisfied, but do not ensure second order accuracy (although the limiters used are second order). Nevertheless, the results presented below prove strong improvement on accuracy when compared with the first order scheme.

Copyright © 2003 John Wiley & Sons, Ltd.

Following from (15) we get

$$\begin{aligned} u_{i+1/2} &= \frac{1}{2}(u_i + u_{i+1}) - \frac{1}{2c_k}(v_{i+1} - v_i) + \frac{\Delta x}{4c_k}(s_i^+ + s_{i+1}^-) \\ v_{i+1/2} &= \frac{1}{2}(v_i + v_{i+1}) - \frac{c_k}{2}(u_{i+1} - u_i) + \frac{\Delta x}{4}(s_i^+ - s_{i+1}^-) \end{aligned} \tag{19}$$

Then the second order (in space) semi-discrete relaxation scheme is given componentwise as

$$\begin{aligned} &\frac{\partial}{\partial t}u_i + \frac{1}{2\Delta x}(v_{i+1} - v_{i-1}) - \frac{c_k}{2\Delta x}(u_{i+1} - 2u_i + u_{i-1}) \\ &\quad - \frac{1}{4}(s_{i+1}^- - s_i^- + s_{i-1}^+ - s_i^+) = 0 \\ &\frac{\partial}{\partial t}v_i + \frac{c_k^2}{2\Delta x}(u_{i+1} - u_{i-1}) - \frac{c_k}{2\Delta x}(v_{i+1} - 2v_i + v_{i-1}) \\ &\quad + \frac{c_k}{4}(s_{i+1}^- - s_i^- - s_{i-1}^+ + s_i^+) = -\frac{1}{\varepsilon}(v_i - F_k(u_i)) - \frac{1}{\varepsilon}\tilde{S}_k(u_i) \end{aligned} \tag{20}$$

with $\tilde{S}_k, F_k$ being the kth components of $\tilde{\mathbf{S}}, \mathbf{F}$, respectively. Notice that in the case the slope $s^{\pm} = 0$ or $\phi = 0$, the MUSCL scheme (20) reduces to the upwind scheme (14).

4. FULLY DISCRETE SCHEMES

In this section we present the time discretization of the semi-discrete relaxation schemes applied to the SW equations. We will compare the two space discretizations, upwind and MUSCL, applying an implicit Runge–Kutta method as the time marching mechanism to advance the solution by one time step Δt. To simplify the presentation we assume that $Z \equiv 0$, then

(A) Given $\mathbf{u}^n, \mathbf{v}^n$ apply a finite volume method to update $\mathbf{u}, \mathbf{v}$ over time Δt by solving the homogeneous linear hyperbolic system

$$\begin{bmatrix} \mathbf{u} \\ \mathbf{v} \end{bmatrix}_t + \begin{bmatrix} 0 & \mathbf{I} \\ \mathbf{C}^2 & 0 \end{bmatrix} \begin{bmatrix} \mathbf{u} \\ \mathbf{v} \end{bmatrix}_x = \begin{bmatrix} 0 \\ 0 \end{bmatrix} \tag{21}$$

and obtain new values $\mathbf{u}^{(1)}, \mathbf{v}^{(1)}$.

(B) Update $\mathbf{u}^{(1)}, \mathbf{v}^{(1)}$ to $\mathbf{u}^{n+1}, \mathbf{v}^{n+1}$ by solving the equations

$$\mathbf{u}_t = 0 \tag{22}$$

$$\mathbf{v}_t = -\frac{1}{\varepsilon}(\mathbf{v} - \mathbf{F}(\mathbf{u})) \tag{23}$$

over time Δt.

A second order implicit Runge–Kutta (RK) splitting scheme was introduced in Reference [14] and is utilized here for both source term formulations. The splitting treats, alternatively,

Copyright © 2003 John Wiley & Sons, Ltd.

the stiff source terms implicitly in two steps and the convection terms with two explicit steps. Notice that, the space time discretizations are treated separately using what has become known as the method of lines.

For the first source term application, corresponding to system (7), and temporarily dropping the subscript indices, given $\{\mathbf{u}^n, \mathbf{v}^n\}$, $\{\mathbf{u}^{n+1}, \mathbf{v}^{n+1}\}$ are computed by

$$\mathbf{u}^{n,1} = \mathbf{u}^n \tag{24a}$$

$$\mathbf{v}^{n,1} = \mathbf{v}^n + \frac{\Delta t}{\varepsilon}(\mathbf{v}^{n,1} - \mathbf{F}(\mathbf{u}^{n,1})) \tag{24b}$$

$$\mathbf{u}^{(1)} = \mathbf{u}^{n,1} - \Delta t D_+ \mathbf{v}^{n,1} + \Delta t \mathbf{S}(\mathbf{u}^{n,1}) \tag{24c}$$

$$\mathbf{v}^{(1)} = \mathbf{v}^{n,1} - \Delta t \mathbf{C}^2 D_+ \mathbf{u}^{n,1} \tag{24d}$$

$$\mathbf{u}^{n,2} = \mathbf{u}^{(1)} \tag{24e}$$

$$\mathbf{v}^{n,2} = \mathbf{v}^{(1)} - \frac{\Delta t}{\varepsilon}(\mathbf{v}^{n,2} - \mathbf{F}(\mathbf{u}^{n,2})) - \frac{2\Delta t}{\varepsilon}(\mathbf{v}^{n,1} - \mathbf{F}(\mathbf{u}^{n,1})) \tag{24f}$$

$$\mathbf{u}^{(2)} = \mathbf{u}^{n,2} - \Delta t D_+ \mathbf{v}^{n,2} + \Delta t \mathbf{S}(\mathbf{u}^{n,2}) \tag{24g}$$

$$\mathbf{v}^{(2)} = \mathbf{v}^{n,2} - \Delta t \mathbf{C}^2 D_+ \mathbf{u}^{n,2} \tag{24h}$$

$$\mathbf{u}^{n+1} = \tfrac{1}{2}(\mathbf{u}^n + \mathbf{u}^{(2)}) \tag{24i}$$

$$\mathbf{v}^{n+1} = \tfrac{1}{2}(\mathbf{v}^n + \mathbf{v}^{(2)}) \tag{24j}$$

where

$$D_+ \mathbf{w}_i = \frac{1}{\Delta x}(\mathbf{w}_{i+1/2} - \mathbf{w}_{i-1/2})$$

Further in the case of system (9) with the source term present, we get

$$\mathbf{u}^{n,1} = \mathbf{u}^n \tag{25a}$$

$$\mathbf{v}^{n,1} = \mathbf{v}^n + \frac{\Delta t}{\varepsilon}(\mathbf{v}^{n,1} - \mathbf{F}(\mathbf{u}^{n,1})) + \frac{\Delta t}{\varepsilon}\tilde{\mathbf{S}}(\mathbf{u}^{n,1}) \tag{25b}$$

$$\mathbf{u}^{(1)} = \mathbf{u}^{n,1} - \Delta t D_+ \mathbf{v}^{n,1} \tag{25c}$$

$$\mathbf{v}^{(1)} = \mathbf{v}^{n,1} - \Delta t \mathbf{C}^2 D_+ \mathbf{u}^{n,1} \tag{25d}$$

$$\mathbf{u}^{n,2} = \mathbf{u}^{(1)} \tag{25e}$$

$$\begin{aligned}\mathbf{v}^{n,2} = \mathbf{v}^{(1)} &- \frac{\Delta t}{\varepsilon}(\mathbf{v}^{n,2} - \mathbf{F}(\mathbf{u}^{n,2})) \\ &- \frac{2\Delta t}{\varepsilon}(\mathbf{v}^{n,1} - \mathbf{F}(\mathbf{u}^{n,1})) - \frac{\Delta t}{\varepsilon}\tilde{\mathbf{S}}(\mathbf{u}^{n,2}) - \frac{2\Delta t}{\varepsilon}\tilde{\mathbf{S}}(\mathbf{u}^{n,1})\end{aligned} \tag{25f}$$

Copyright © 2003 John Wiley & Sons, Ltd.

$$\mathbf{u}^{(2)} = \mathbf{u}^{n,2} - \Delta t D_+ \mathbf{v}^{n,2} \tag{25g}$$

$$\mathbf{v}^{(2)} = \mathbf{v}^{n,2} - \Delta t \mathbf{C}^2 D_+ \mathbf{u}^{n,2} \tag{25h}$$

$$\mathbf{u}^{n+1} = \tfrac{1}{2}(\mathbf{u}^n + \mathbf{u}^{(2)}) \tag{25i}$$

$$\mathbf{v}^{n+1} = \tfrac{1}{2}(\mathbf{v}^n + \mathbf{v}^{(2)}) \tag{25j}$$

It is worth noting here that, using the above schemes neither linear algebraic equation nor nonlinear source terms arise. In addition the first order relaxation scheme is stable under the usual CFL condition,

$$\max\{c_1, c_2\}\frac{\Delta t}{\Delta x} \leqslant 1 \tag{26}$$

while the second order MUSCL relaxation scheme is TVD (see References [14, 24, 20]) under the additional restriction on CFL,

$$\max\{c_1, c_2\}\frac{\Delta t}{\Delta x} \leqslant \frac{1}{2} \tag{27}$$

The time discretization in the limit when $\varepsilon \to 0$ converges to the TVD Runge–Kutta schemes is given in Reference [32].

5. NUMERICAL TESTS AND RESULTS

We present results of a series of numerical experiments illustrating the various features of the schemes. For consistency in all the experiments reported here the time step Δt was computed according to the condition (27), but in practice higher values can also be used in most calculations.

The choices of c_1 and c_2 in all the numerical tests are based on rough estimates of the two eigenvalues $(u+\sqrt{gh}, u-\sqrt{gh})$ of the original SW equations. Thus, we take $c_1 \geqslant \sup|u+\sqrt{gh}|$ and $c_2 \geqslant \sup|u-\sqrt{gh}|$, which satisfy the subcharacteristic condition (10). Other choices can be made, for example one can simply set $c_1 = c_2 = \max(\sup|u+\sqrt{gh}|, \sup|u-\sqrt{gh}|)$, as long as numerical stability is maintained. It should be noted here that larger c_1, c_2 values usually add more numerical viscosity. The schemes presented here can be viewed as a whole class of schemes depending on the parameters c_1, c_2.

The relaxation parameter ε should be small with respect to the time step and space mesh length, that is $\Delta t \gg \varepsilon$ and $\Delta x \gg \varepsilon$. Again here, ε plays the role of viscosity coefficient so more numerical diffusion will be added for relatively larger values of ε, see Reference [19] for a discussion on this matter.

5.1. Dam break flow

In order to check the validity and behaviour of the relaxation schemes we first consider a non-stationary case, the dam break problem in a rectangular channel with flat bottom, $Z = 0$.

Copyright © 2003 John Wiley & Sons, Ltd.

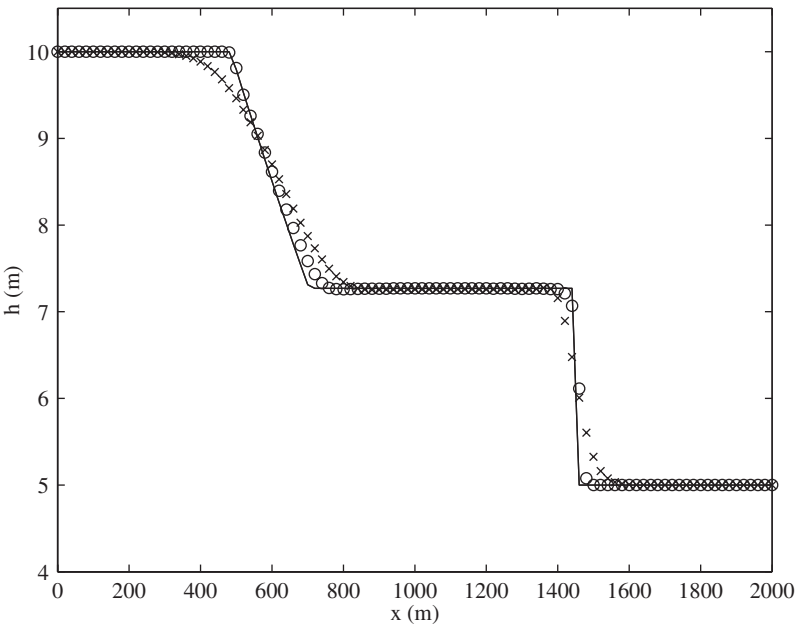

Figure 2. Dam-break flow, $h_0/h_1 = 0.5$, $\Delta x = 20$ m, $c_1 = 5$, $c_2 = 12$, ($\times$) Upwind and ($\circ$) MUSCL with MC limiter.

We computed the solution on a channel of length $L = 2000$ m for time $T = 50$ s and with initial conditions:

$$u(x,0) = 0$$

$$h(x,0) = \begin{cases} h_1 & x \leqslant 1000 \\ h_0 & x > 1000 \end{cases}$$

with $h_1 > h_0$. This is the corresponding Riemann problem for the homogeneous problem. The water depth ratio is given by h_0/h_1. The dam collapses at $t = 0$ and the resulting flow consists of a shock wave (bore) travelling downstream and a rarefaction wave (depression wave) travelling upstream. The upstream depth h_1 was kept constant at 10 m, while the downstream depth h_0 was different for each problem. When the depth ratio is greater than 0.5, the flow throughout the channel remains subcritical. For depth ratios smaller than 0.5, the flow downstream of the dam position is supercritical while remaining subcritical upstream. For very small values of the ratio h_0/h_1 the flow regime becomes strongly supercritical downstream and the shock wave can be difficult to capture. The analytical (exact) solutions for these sample problems were calculated using Stoker's [33] method and shown as a solid line in the all the figures. The values used were $\varepsilon = 1.E-4$ and CFL $= 0.5$.

The results presented in Figures 2–5 for the water height profile compare well with the analytical solution. The discontinuities are correctly captured and the shock strength is predicted accurately without the use of a very fine grid (as in Figure 3). The performance of the MUSCL relaxing scheme is superior, as expected, compared to the upwind one, especially

Copyright © 2003 John Wiley & Sons, Ltd.

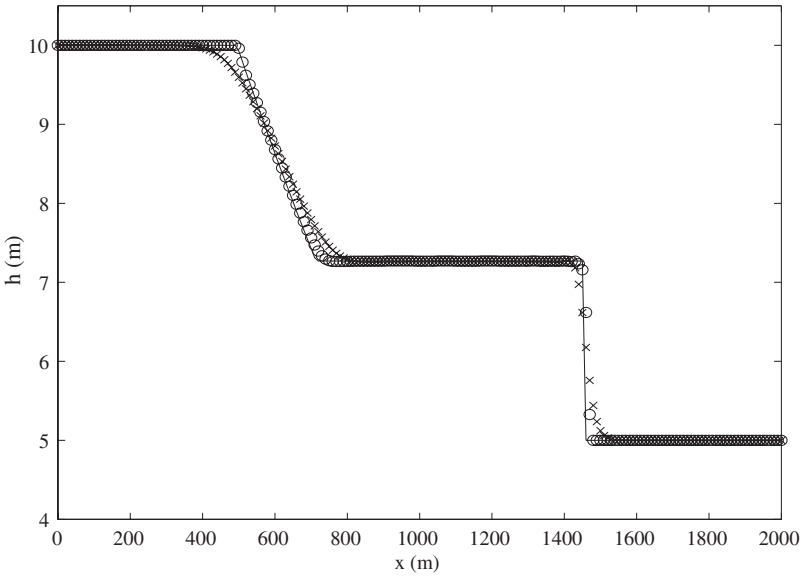

Figure 3. Dam-break flow, $h_0/h_1 = 0.5$, $\Delta x = 10$ m, $c_1 = 5$, $c_2 = 12$, ($\times$) Upwind and ($\circ$) MUSCL with MC limiter.

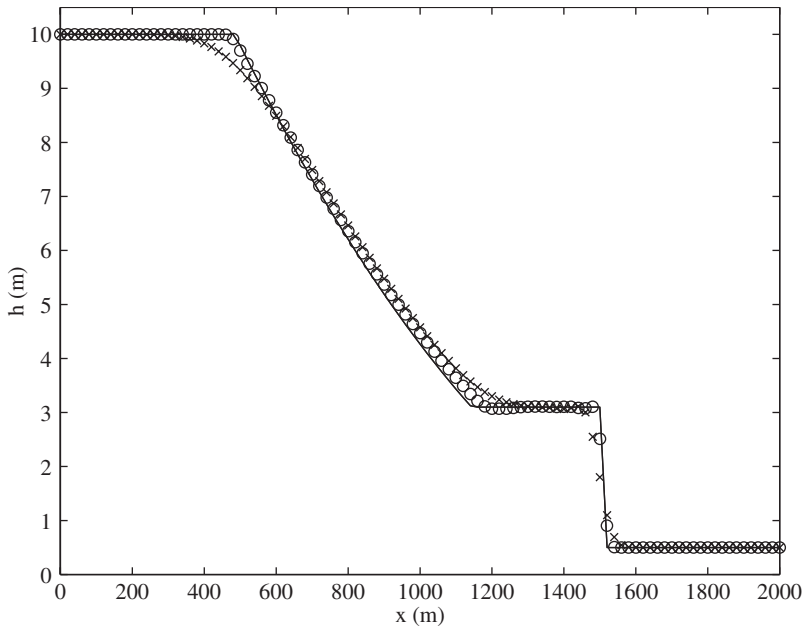

Figure 4. Dam-break flow, $h_0/h_1 = 0.05$, $\Delta x = 20$ m, $c_1 = 6$, $c_2 = 16$, ($\times$) Upwind and ($\circ$) MUSCL with MC limiter.

Copyright © 2003 John Wiley & Sons, Ltd.

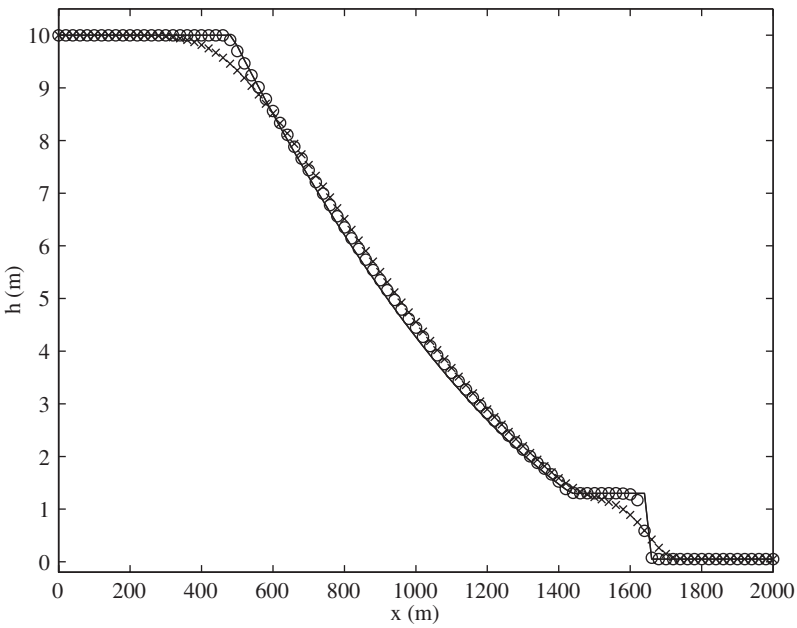

Figure 5. Dam-break flow, $h_0/h_1 = 0.005$, $\Delta x = 20$ m, $c_1 = 12$, $c_2 = 18$, ($\times$) Upwind and ($\circ$) MUSCL with MC limiter.

for the smallest depth ratio. The results compare very well to the solutions obtained by more classical methods (such as approximate Riemann solvers and TVD methods), for the same problem (see for example References [34, 35]).

In Figures 6 and 7 the results for the smaller depth ratios for the MUSCL relaxation scheme presented in Figures 4 and 5 are compared with the classical second order in space explicit MUSCL scheme (see Reference [34]) for the same computational parameters and limiter. The results are similar especially for the shock calculation in Figure 6 while the classical MUSCL scheme is proven slightly more diffusive on the head and tail of the rarefaction wave.

5.1.1. Dry bed problem. For the next test problem, we consider a dry bed on the downstream of the dam ($h_0 = 0$). For brevity results are presented only for the MUSCL relaxing scheme and compared with the analytical solutions at time $T = 40$ s in Figures 8–10. This is a challenging numerical problem as a result of the singularity that occurs at the transition point of the advancing front. The computed solution for h follows closely the analytical one, the transition point between the wet and the dry zone is close to the exact one, but some difficulties appear on the velocity. Indeed, as the solution is similar to a peak in this zone, the TVD scheme becomes of order 1 and is diffusive. Nevertheless, the results are globally accurate and totally non-oscillatory. We also verify numerically that the positivity of the water height and discharge is preserved. From a practical perspective, the overall performance of the MUSCL relaxing scheme is particular attractive because the solution remains stable, monotone and highly accurate (at least away from the wet/dry interface) without requiring special front tracking techniques or deforming grids.

Copyright © 2003 John Wiley & Sons, Ltd.

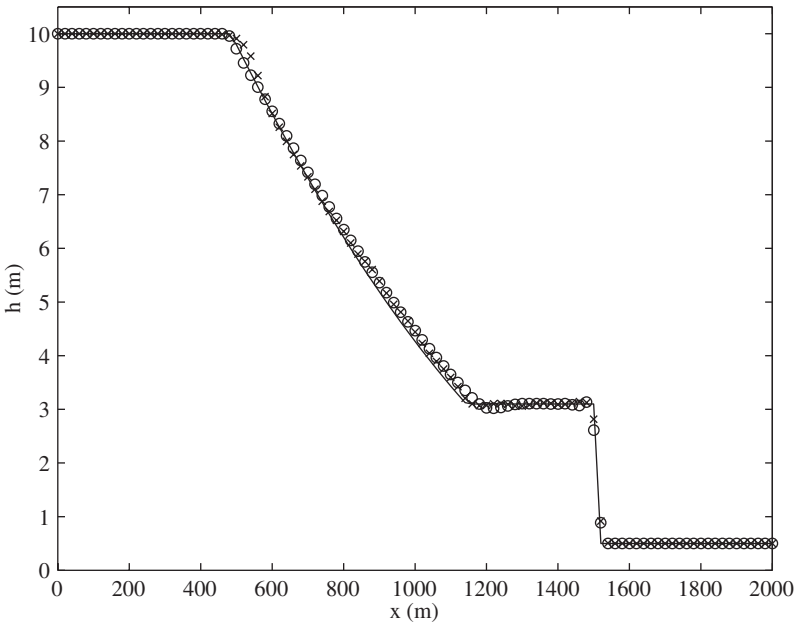

Figure 6. Dam-break flow, $h_0/h_1 = 0.05$, ($\times$) MUSCL (classical) with MC limiter, ($\circ$) MUSCL (relaxation) with MC limiter.

5.2. Flow at rest

We consider system (1) with initial conditions

$$u(x,0) = 0, \quad \forall x \in \mathbb{R}$$
$$h(x,0) + Z(x) = H, \quad \forall x \in \mathbb{R}$$

then clearly

$$u(x,t) = 0, \quad \forall x \in \mathbb{R},\ t \geqslant 0$$
$$h(x,t) + Z(x) = H, \quad \forall x \in \mathbb{R},\ t \geqslant 0$$

is a solution to (1).

We test our scheme to this steady state flow where the bathymetry is non-trivial and is given by

$$Z(x) = \begin{cases} 0.2 - 0.05(x-10)^2, & 8 \leqslant x \leqslant 12 \\ 0, & \text{otherwise} \end{cases} \tag{28}$$

in channel of length $L = 25\,\text{m}$ and $H = 2\,\text{m}$, $\varepsilon = 1.E-5$, $c_1 = 4, c_2 = 4.5$ and $\text{CFL} = 0.5$. Figures 11 and 12 display the final water level and the final unit discharge values respectively, for the MUSCL schemes (24) and (25) at time $T = 200\,\text{s}$ and mesh size $\Delta x = 0.125\,\text{m}$ and with

Copyright © 2003 John Wiley & Sons, Ltd.

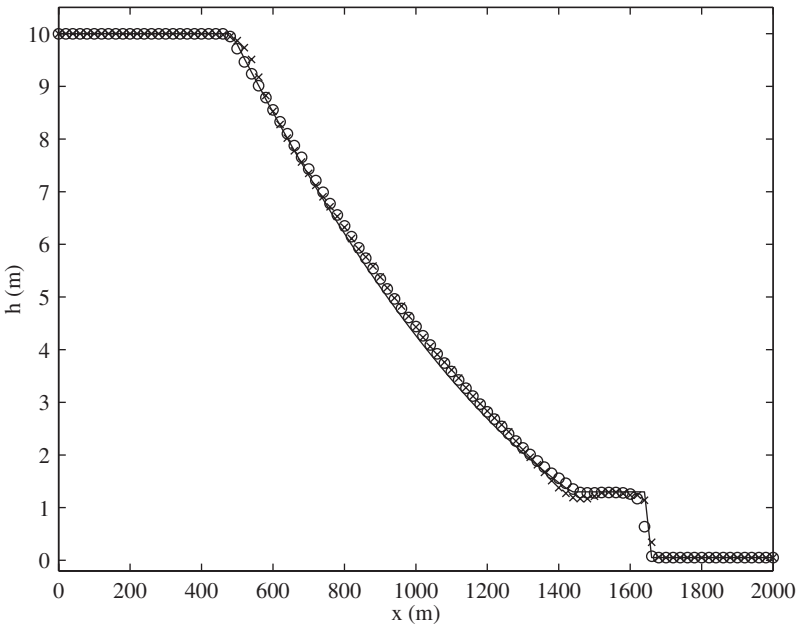

Figure 7. Dam-break flow, $h_0/h_1 = 0.005$, ($\times$) MUSCL (classical) with MC limiter, ($\circ$) MUSCL (relaxation) with MC limiter.

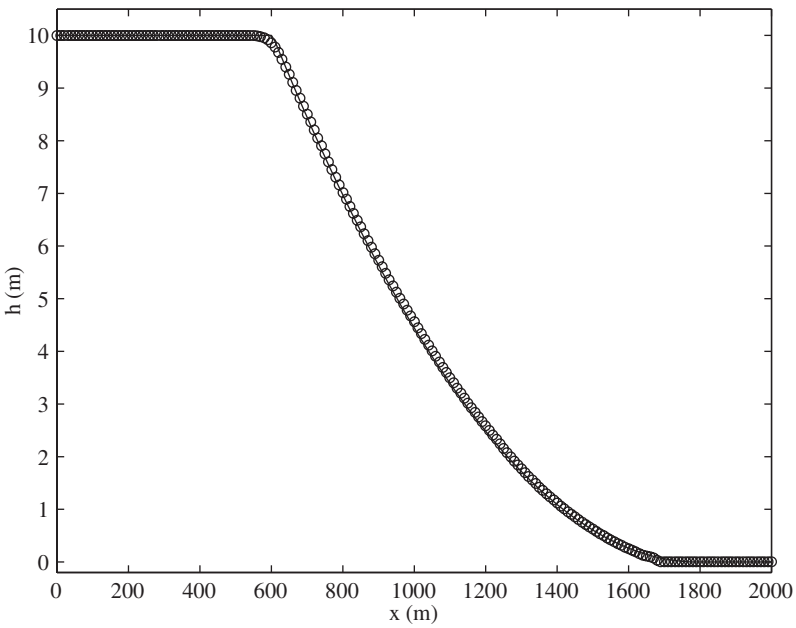

Figure 8. Dry bed dam-break flow (h), $\Delta x = 10\,\mathrm{m}$, $c_1 = 18$, $c_2 = 16$, ($\circ$) MUSCL with MM limiter.

Copyright © 2003 John Wiley & Sons, Ltd.

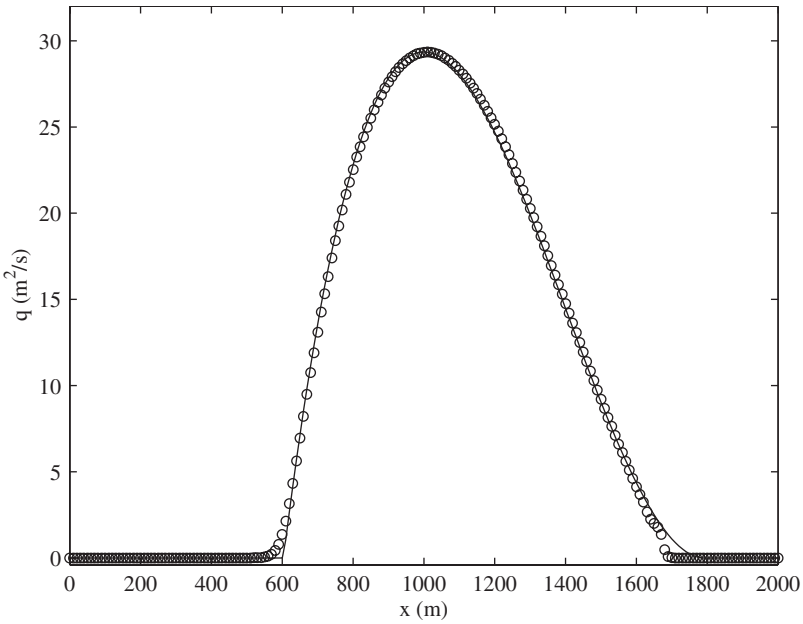

Figure 9. Dry bed dam-break flow (q), $\Delta x = 10\,\mathrm{m}$, $c_1 = 18$, $c_2 = 16$, ($\circ$) MUSCL with MM limiter.

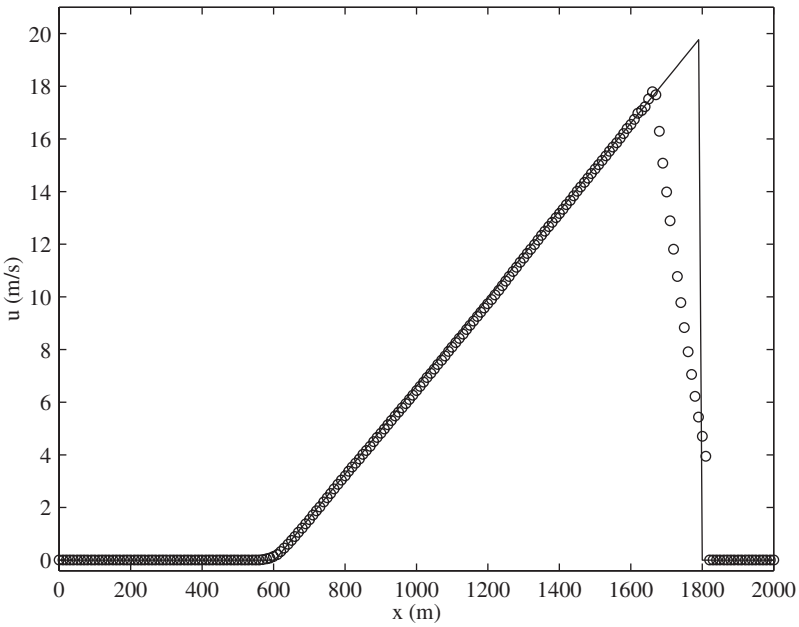

Figure 10. Dry bed dam-break flow (u), $\Delta x = 10\,\mathrm{m}$, $c_1 = 18$, $c_2 = 16$, ($\circ$) MUSCL with MM limiter.

Copyright © 2003 John Wiley & Sons, Ltd.

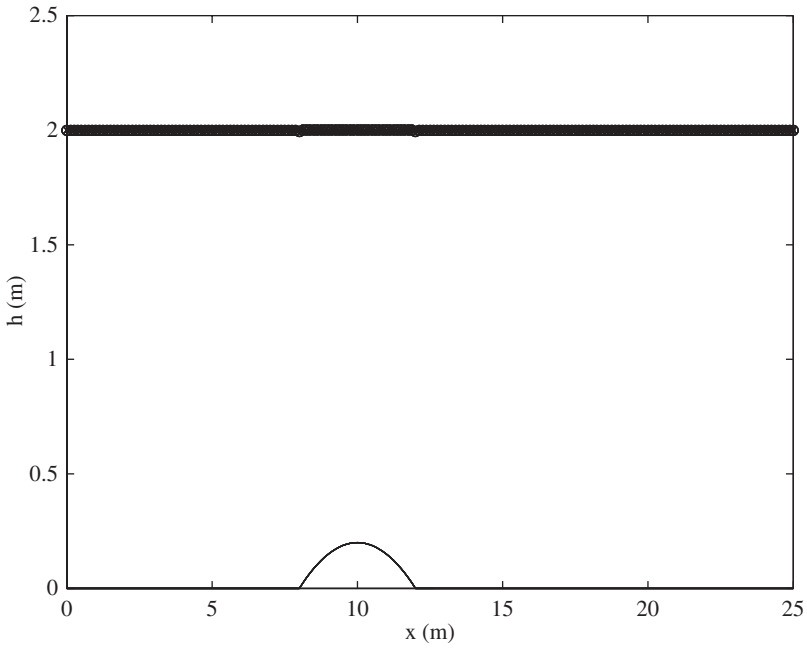

Figure 11. Flow at rest (water height): (+) scheme (24) and (∘) scheme (25).

the same computational parameters used. In all the figures the theoretical (exact) solution is represented with a solid line.

We notice the difference between the two schemes (based on the treatment of the source term), especially the discharge for scheme (24) converges to an oscillatory solution as one can see with closer inspection in Figure 13, while the result for (25) was almost to machine accuracy away from the hump.

The variance of the values of the water level as well as of the discharge from the steady states for scheme (25) (as $\varepsilon \to 0$) are of $O(\varepsilon)$ as can be seen in Table I. For consistency we have used the same CFL number for the results presented in Table I, up to the value of ε where $\Delta t \neq O(\varepsilon)$. We should stress here that, as noted before, for the relaxation schemes presented $\Delta t \gg \varepsilon$.

In Figures 14 and 15 we compare scheme (25) with Roe's scheme with upwinding of the source terms (see References [8, 10]). Away from the hump both schemes give indistinguishable solution (close to machine accuracy) while Roe's scheme performs slightly better (as can be seen in the magnified view in Figure 15) on the hump region, this is due to the discritizations performed, designed to preserve such steady states.

5.3. *Steady flow over a hump*

In this benchmark test case we study the convergence towards steady flow over a hump, (28) and the same length as before. Depending on the initial and boundary conditions, the flow may be subcritical, transcritical with a shock or without a shock. Computational parameters

Copyright © 2003 John Wiley & Sons, Ltd.

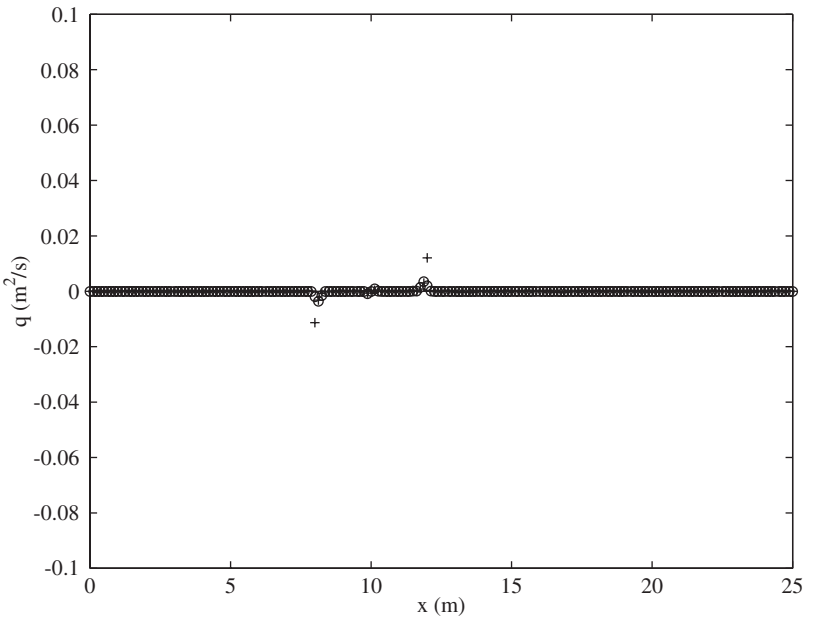

Figure 12. Flow at rest (discharge): (+) scheme (24) and (∘) scheme (25).

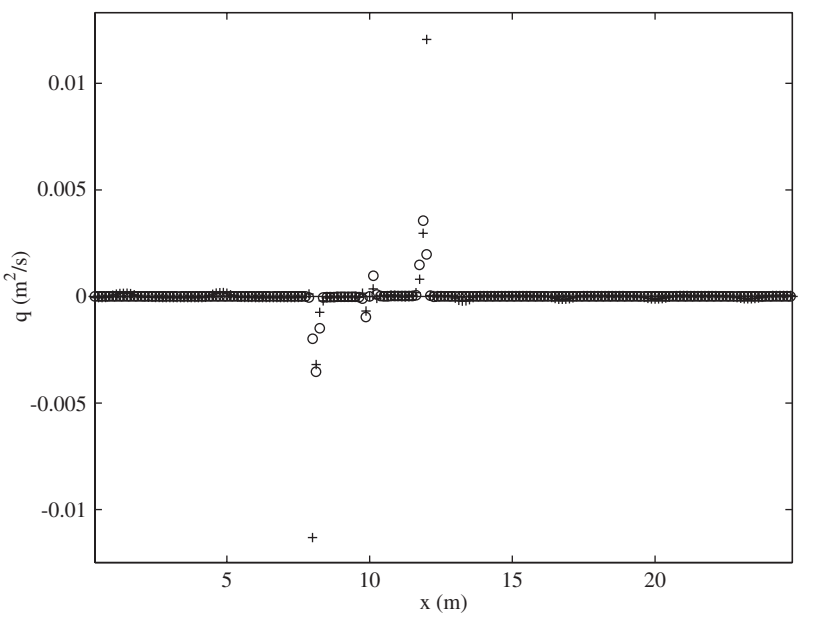

Figure 13. Flow at rest: Magnified view of Figure 12 for the discharge.

Copyright © 2003 John Wiley & Sons, Ltd.

Table I. ℓ_1 errors for the water at rest problem (CFL = 0.5).

ε	ℓ_1 error for h	Rate(h)	ℓ_1 error for q	Rate(q)
$1.E-1$	$3.212E-3$	—	$2.327E-2$	—
$8.E-2$	$2.271E-3$	1.551	$1.921E-2$	0.860
$6.E-2$	$1.425E-3$	1.619	$1.478E-2$	0.908
$4.E-2$	$7.383E-4$	1.628	$1.000E-2$	0.954
$2.E-2$	$2.646E-4$	1.480	$5.154E-3$	0.962

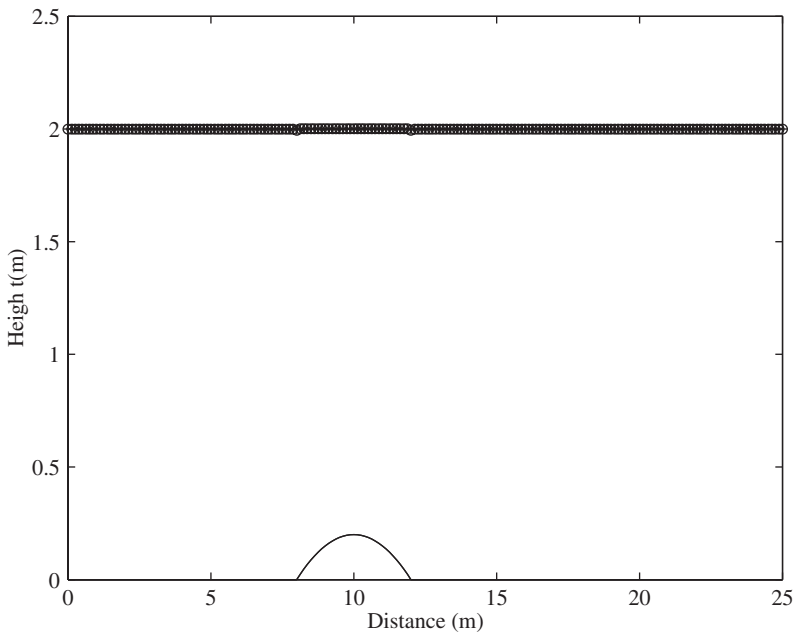

Figure 14. Flow at rest: (○) scheme (25) and (×) Roe scheme (with source term upwinding).

common for all three cases are: CFL = 0.5, $\Delta x = 0.125$ m, $T = 200$ s. The initial conditions in all cases are taken to be

$$u(x,0) = 0$$

$$h(x,0) + Z(x) = H_0$$

where H_0 is the constant water level downstream provided by the boundary condition. For brevity results are presented only for the MUSCL scheme (25), with the improved inclusion of the source term, and using the MC limiter. In each test case the results are compared with the exact solution which is presented as a solid line.

5.3.1. Subcritical flow. We impose an upstream boundary condition for the discharge $q = 4.42\ \mathrm{m}^2/\mathrm{s}$ and a downstream boundary condition for the water level $H_0 = 2$ m. The com-

Copyright © 2003 John Wiley & Sons, Ltd.

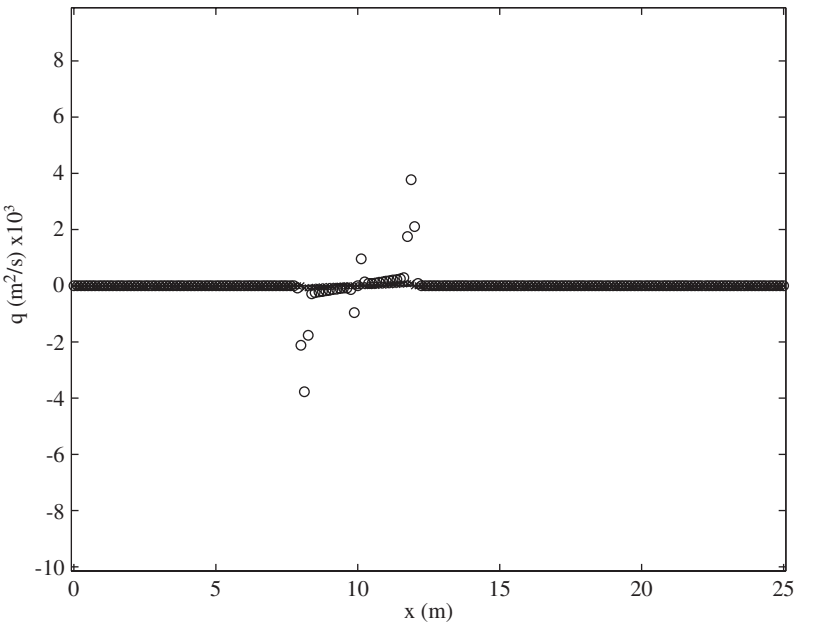

Figure 15. Flow at rest: (○) scheme (25) and (×) Roe scheme (with source term upwinding).

putational parameters were $\varepsilon = 1.E-5$, $c_1 = 4$ and $c_2 = 7$. The final water level as well as the discharge are displayed in Figures 16 and 17.

5.3.2. Transcritical flow without shock. In this case we impose an upstream boundary condition for the discharge $q = 1.53\,\mathrm{m}^2/\mathrm{s}$ and a downstream boundary condition for the water level $H_0 = 0.66\,\mathrm{m}$ only in the case where the flow is subcritical. If the flow becomes supercritical downstream, no condition for the water level is imposed. The computational parameters were $\varepsilon = 1.E-5$, $c_1 = 5$ and $c_2 = 6$. The final water level as well as the discharge are displayed in Figures 18 and 19.

5.3.3. Transcritical flow with shock. In this test case the upstream boundary condition for the discharge is $q = 0.18\,\mathrm{m}^2/\mathrm{s}$ and the downstream boundary condition for the water level is $H_0 = 0.33\,\mathrm{m}$. The computational parameters were $\varepsilon = 1.E-6$ and $c_1 = c_2 = 5$. The final water level as well as the discharge are displayed in Figures 20 and 21, where they compared with the analytical solutions and that of the Roe scheme with source term upwinding.

5.3.4. Drain on a non-flat bottom. This is a difficult problem for all numerical methods, since it involves the calculation of dry areas and it has been proposed in Reference [6]. With the same topography as before, we consider the channel draining off and we assume that the upstream boundary condition is a 'mirror state'-type (reflective) and the downstream boundary condition is that of a dry bed. The initial condition is set to $h + Z = 0.5\,\mathrm{m}$ and $q = 0\,\mathrm{m}^3/\mathrm{s}$. The solution for this test case ($t = +\infty$) is a state at rest, on the left part of the hump with

Copyright © 2003 John Wiley & Sons, Ltd.

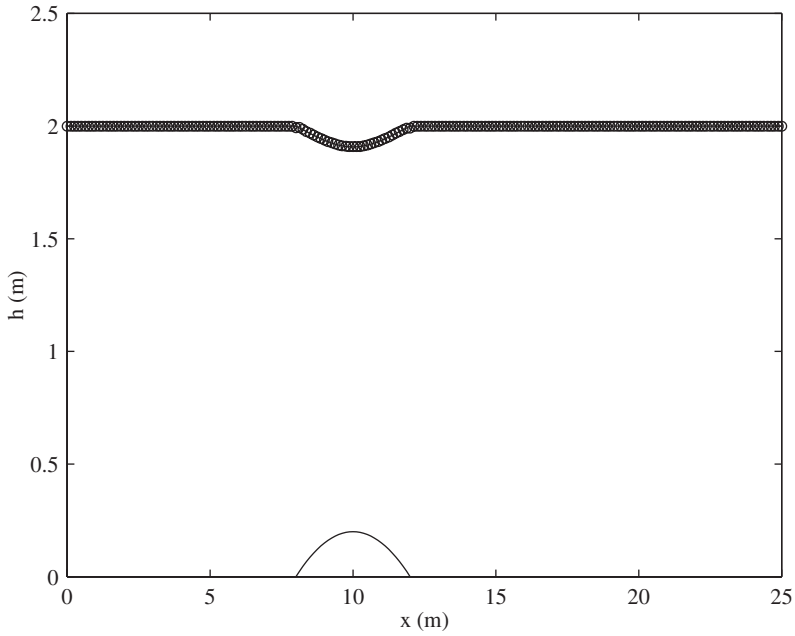

Figure 16. Subcritical flow over a hump (h).

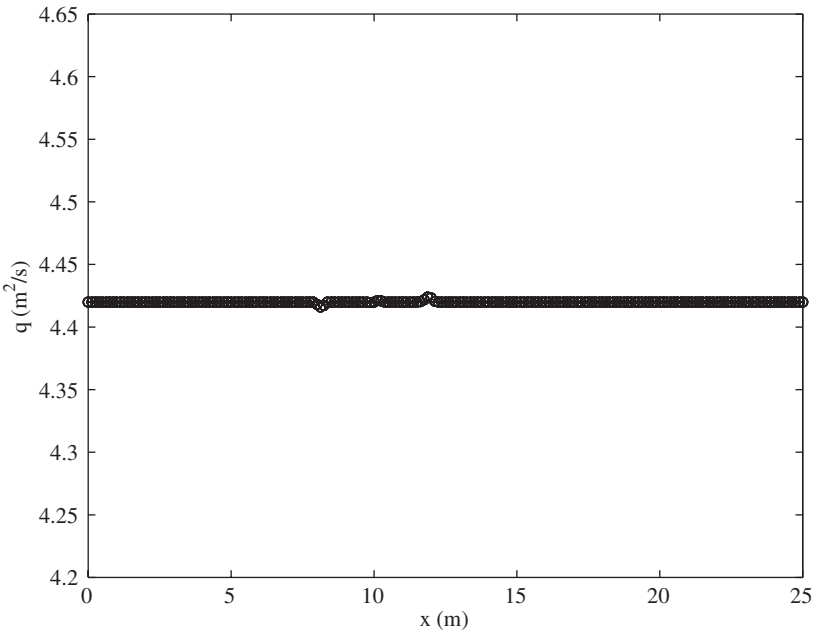

Figure 17. Subcritical flow over a hump (q).

Copyright © 2003 John Wiley & Sons, Ltd.

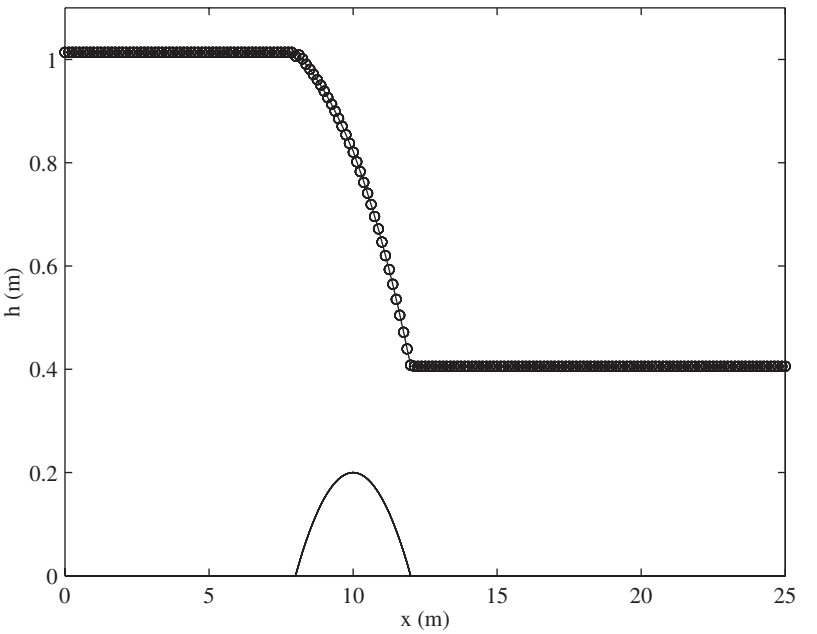

Figure 18. Transcritical flow over a hump (h).

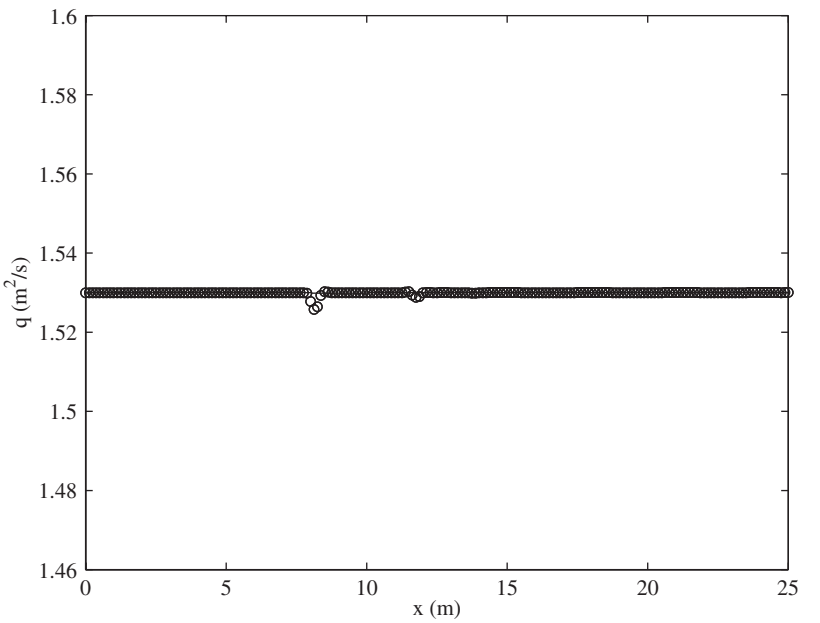

Figure 19. Transcritical flow over a hump (q).

Copyright © 2003 John Wiley & Sons, Ltd.

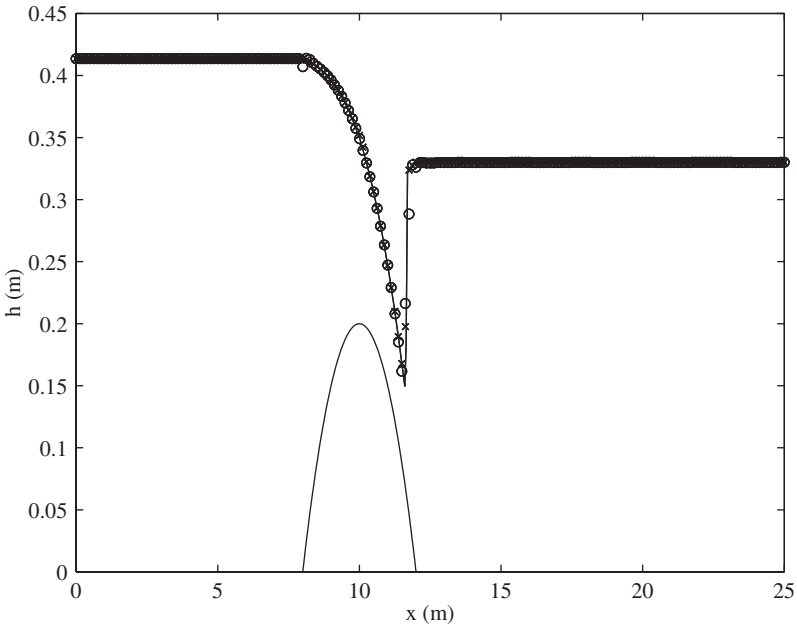

Figure 20. Transcritical flow with shock: (○) scheme (25) and (×) Roe scheme (with source term upwinding).

$h+Z=0.2$ m with $q=0\,\mathrm{m}^3/\mathrm{s}$ and a dry state (i.e. $h=0$ and $q=0\,\mathrm{m}^3/\mathrm{s}$) on the right of the hump.

The depth and discharge profiles were calculated at several times $t=10, 20, 100, 1000$ s with a 250 uniform grid and CFL $=0.5$ and presented in Figures 22 and 23. The computational parameters were $\varepsilon=1.E-6$ and $c_1=c_2=3.5$. The proposed model converges to the expected steady state solution, as it can be seen in Figures 22 and 23. It is important to notice here that the results were obtained without any modification of the method to overcome the dry area problem of zero depth and discharge and compare well with those presented in References [6, 36].

In all the four test problems presented above the results compare well the analytical solutions and with already published solutions (see for example References [6, 9]), converging to the correct steady state solutions without any unwanted oscillations.

6. CONCLUSIONS

In the present work relaxation schemes have been studied in order to compute shallow water flows with and without a topography source term present. The main feature of the schemes is their simplicity and robustness. Finite volume shock capturing spatial discretizations, that are Riemann solver free, have been used providing accurate shock resolution. A new way to incorporate the topography source term was applied with the relaxation model and only small errors were introduced while preserving steady states. The benchmark tests have shown

Copyright © 2003 John Wiley & Sons, Ltd.

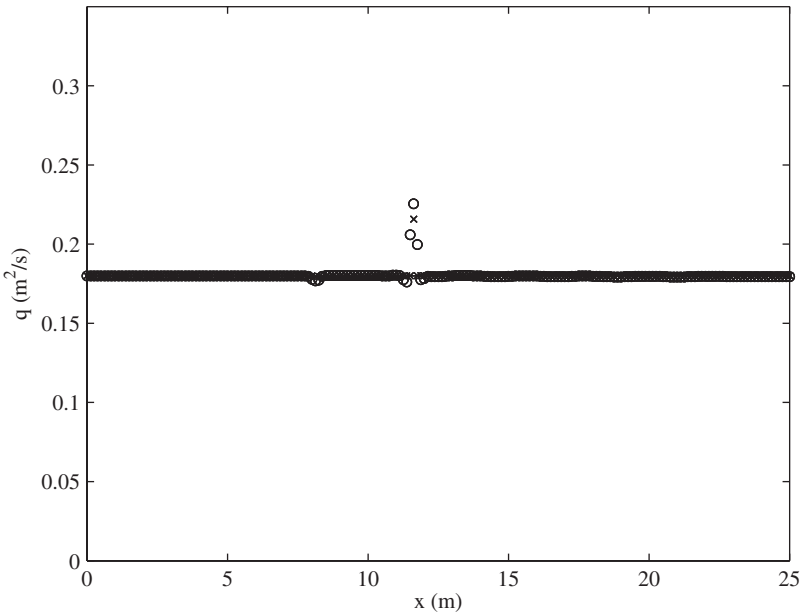

Figure 21. Transcritical flow with shock: (○) scheme (25) and (×) Roe scheme (with source term upwinding).

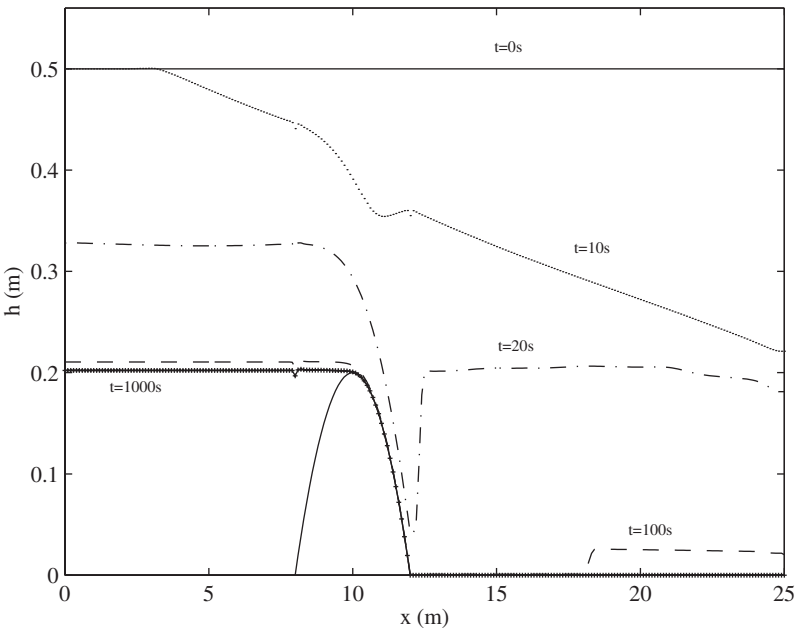

Figure 22. Drain on a non-flat bottom (h).

Copyright © 2003 John Wiley & Sons, Ltd.

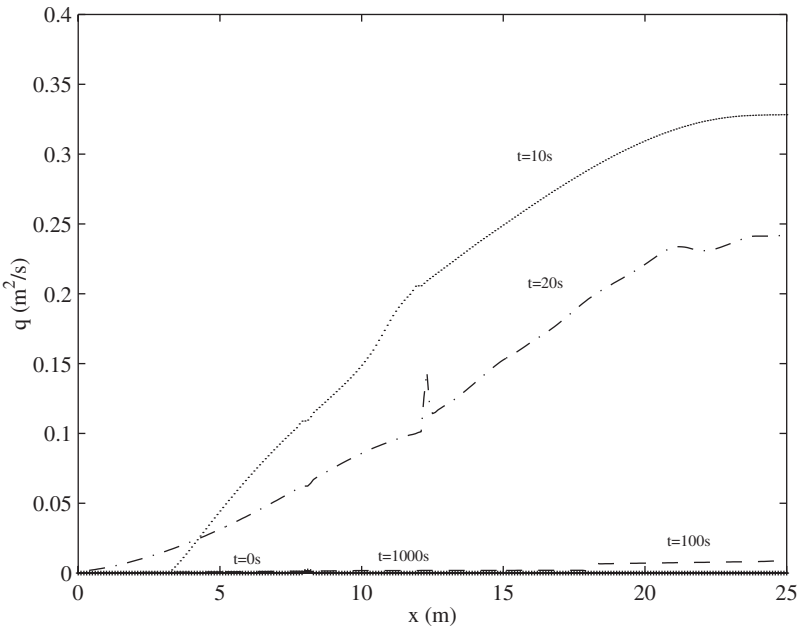

Figure 23. Drain on a non-flat bottom (q).

that the schemes provide accurate solutions in good agreement with well known analytical solutions. The results also demonstrate that relaxation schemes are accurate, simple, efficient and robust and can be of practical consideration when solving shallow water flow problems involving bed slope source terms. In addition, work to extend the relaxation schemes to the two dimensional SW equations is underway.

ACKNOWLEDGEMENTS

The authors wish to thank Prof. Ch. Makridakis for his valuable help and Prof. S. Jin for bringing in to our attention the work in Reference [23]. We also thank the reviewers for their valuable comments.

REFERENCES

1. Greenberg JM, LeRoux AY. A well-balanced scheme for the numerical processing of source terms in hyperbolic equations. *SIAM Journal of Numerical Analysis* 1996; **33**:1–16.
2. Gosse L, LeRoux AY. A well-balanced scheme designed for inhomogeneous scalar conservation laws. *Comptes Rendus des Seances de l'Academie des Sciences*, *Serie I Mathematique* 1996; **323**:543–546.
3. Gosse L. A well-balanced flux vector splitting scheme designed for hyperbolic systems of conservation laws with source terms. *Computational Mathematics and Application* 2000; **39**:135–159.
4. Gosse L. A well balanced scheme using non-conservative products designed for hyperbolic systems of conservation laws with source terms. *Mathematical Modelling and Methods in Applied Science* 2001; **11**: 339–366.
5. Jin S. A steady-state capturing method for hyperbolic systems with geometrical source terms. *Mathematical Modelling and Numerical Analysis* 2001; **35**:631–646.
6. Gallouët T, Herard JM, Seguin N. Some approximate Godunov schemes to compute shallow water equations with topography. *Computers and Fluids* 2003; **32**:479–513.

Copyright © 2003 John Wiley & Sons, Ltd.

7. LeVeque RJ. Balancing source terms and flux gradients in high resolution Godunov methods: the quasi-steady wave propagation algorithm. *Journal of Computational Physics* 1998; **146**:346–365.
8. Bermudez A, Vázquez ME, Upwind methods for hyperbolic conservation laws with source terms. *Computers and Fluids* 1994; **23**:1049.
9. Vázquez-Cendón ME. Improved treatment of source terms in upwind schemes for the shallow water equations in Channels with Irregular Geometry. *Journal of Computational Physics* 1999; **148**:497–526.
10. Garcia-Navarro P, Vázquez-Cendón ME. On numerical treatment of the source terms in the shallow water equations. *Computers and Fluids* 2000; **29**:951–979.
11. Kurganov A, Levy L. Central-upwind schemes for the Saint-Venant system. *Mathematical Modelling and Numerical Analysis* 2002; **36**:397–425.
12. Audusse E, Bristeau MO, Perthame B. Kinetic schemes for Saint-Venant equations with source terms on unstructured grids. *INRIA Report RR-3989*, 2000.
13. Perthame B, Simeoni C. A kinetic scheme for the Saint-Venant system with a source term. *Calcolo* 2001; **37**:201–231.
14. Jin S, Xin Z. The relaxing schemes of conservations laws in arbitrary space dimensions. *Communications in Pure and Applied Mathematics* 1995; **48**:235–277.
15. Chen GO, Levermore CD, Liu TP. Hyperbolic conservation laws with stiff relaxation terms and entropy. *Communications in Pure and Applied Mathematics* 1994; **47**:787–830.
16. Aregba-Driollet D, Natalini R. Convergence of relaxation schemes for conservation laws. *Applicable Analysis* 1996; **61**:163–193.
17. Liu HL, Warnecke G. Convergence rates for relaxation schemes approximating conservation laws. *SIAM Journal of Numerical Analysis* 2000; **37**:1316–1337.
18. Katsoulakis M, Kossioris G, Makridakis Ch. Convergence and error estimates of relaxation schemes for multidimensional conservation laws. *Communications in Partial Differential Equations* 1999; **24**:395–424.
19. Arvanitis Ch, Katsaounis Th, Makridakis Ch. Adaptive finite element relaxation schemes for hyperbolic conservations laws. *Mathematical Modelling and Numerical Analysis* 2001; **35**:17–33.
20. Tang T, Wang J. Convergence of MUSCL relaxing schemes to the relaxed schemes for conservation laws with stiff Source terms. *Journal of Scientific Computing*, 2000; **15**:173–195.
21. Lattanzio C, Serre D. Convergence of a relaxation scheme for hyperbolic systems of conservation laws. *Numerical Mathematics* 2001; **88**:121–134.
22. LeVeque RJ, Pelanti M. A class of approximated Riemann solvers and their relation to relaxation schemes. *Journal of Computational Physics* 2001; **172**:572–591.
23. Aral MM, Zhang Y, Jin S. Application of relaxation scheme to wave propagation simulation in open-channel networks. *Journal of Hydraulic Engineering* 1998; **124**:1125–1133.
24. Chalabi A. Convergence of relaxation schemes for hyperbolic conservation laws with stiff source terms. *Mathematics of Computers* 1999; **68**:955–970.
25. Katsaounis Th, Makridakis Ch. Adaptive finite element relaxation schemes for the Saint-Venant system. *DMA-02-02*, *ENS*, Paris, France 2002.
26. Chen GO, Liu TP. Zero relaxation and dissipation limits for hyperbolic conservation laws. *Communications in Pure and Applied Mathematics* 1993, **46**:744–781.
27. Liu TP. Hyperbolic conservation laws with relaxation. *Communication in Mathematical Physics* 1987; **108**: 153–175.
28. Natalini R. Convergence to equilibrium for the relaxation approximations of conservation laws. *Communications in Pure and Applied Mathematics* 1996; **49**:795–823.
29. Xu WQ. Relaxation limit for piecewise smooth solutions to systems for conservation laws. *Journal of Differential Equations* 2000; **162**:140–173.
30. Tzavaras AE. Materials with internal variables and relaxation to conservation laws. *Archives of Rational Mechanics and Analysis* 1999; **146**:129–155.
31. Sweby PK. High resolution schemes using flux limiters for hyperbolic conservation laws. *SIAM Journal on Numerical Analysis* 1984; **21**:995–1011.
32. Shu C-W, Osher S. Efficient implementation of essentially nonoscillatory shock-capturing schemes. *Journal of Computational Physics* 1988; **77**:439–471.
33. Stoker JJ. *Water Waves*. Interscience Publishers, Inc., New York, 1986.
34. Delis AI, Skeels CP. TVD schemes for open channel flow. *International Journal for Numerical Methods in Fluids* 1998; **26**:791–809.
35. Delis AI, Skeels CP, Ryrie SC. Evaluation of some approximate Riemann solvers for transient open channel flows. *Journal of Hydraulic Research* 2000; **38**:217–232.
36. Delis AI. Improved application of the HLLE Riemann solver for the shallow water equations with source terms. *Communications in Numerical Methods in Engineering* 2003; **19**:59–83.

Copyright © 2003 John Wiley & Sons, Ltd.